Process Mapping of Laser surface modification of AISI 316L Stainless Steel for biomedical applications

Evans Chikarakara, Sumsun Naher, Dermot Brabazon

Materials Processing Research Centre, Dublin City University, Dublin 9, Ireland

INTRODUCTION

❑ The main material groups dominating in biomedical implants are:
   316L stainless steel, cobalt-chrome-molybdenum alloys, pure titanium and titanium alloys
❑ Mainly due to their strength, wear and corrosion resistance, biocompatibility and cost
❑ Wear debris is an ongoing concern in relation to life of total joint replacements [1,2]
❑ Laser surface modification is currently being studied; advantages over other surface modification techniques include:
- superior bonding   - reduced distortion   - simple oxidation elimination techniques
- easier control over depth of processing [3]
❑ Scanning high power density lasers on a workpiece can cause the heated surface to melt, while varying the exposure time dictates heating and cooling regimes subsequently controlling the resulting surface microstructures
❑ Theoretically, laser treatment of 316L steel can produce an amorphous surface layer if heating and quenching rates are controlled according to the materials specification
❑ Advantages of an amorphous layer include improved hardness, wear and corrosion resistance mainly due to elimination of crystalline anisotropy and inter-crystalline defects [4,5].

PROCESS PARAMETERS

CO$_2$ Laser Specifications		Fixed Parameters		Varied parameters	
Max Peak Power	1.5kW	Tangential Speed	270mm/s	Duty Cycle	15 – 50%
Wavelength	10.6µm	Linear Speed	46mm/s	Peak Power	500 -1500W
Beam Quality	TEM$_{00}$	Overlap	0%	Residence Time	50 – 167µs
Spot size (minimum/used)	90µm	Pulse Repetition Frequency	3kHz	Irradiance	7.9 – 23.6MW/cm^2

EXPERIMENTAL

Sample Preparation
❑ Cylindrical AISI 316L austenitic stainless steel, ~120mm long and 10mm in diameter
❑ Argon gas at 1 bar pressure shielded the melt pool thus avoiding oxidation
❑ The workpiece was rotated with a DC motor fixed to a table moving perpendicular to the laser irradiation direction
❑ The laser beam was kept perpendicular to the workpiece during laser irradiation to maximise the absorbance and ensure uniform conditions for processing [6]
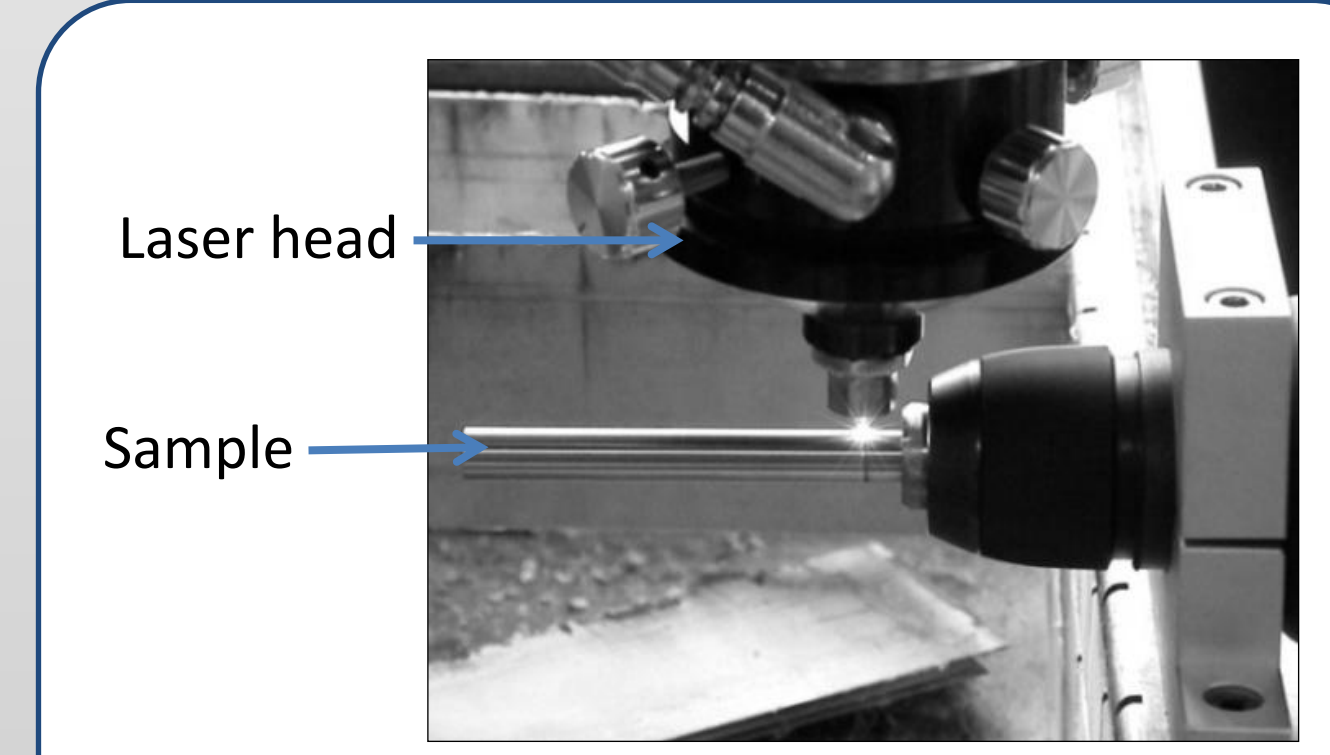
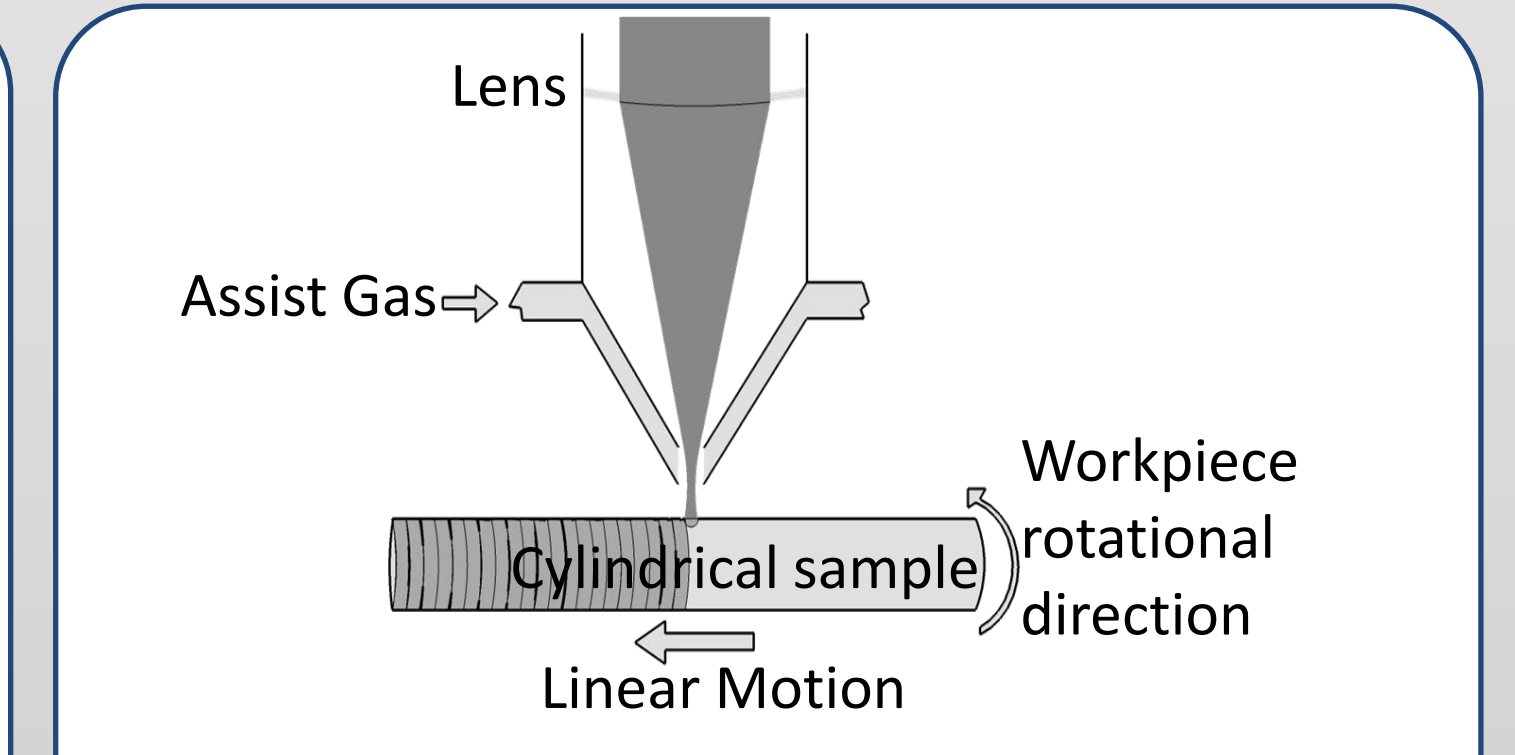
Figure 1: Image of the laser processing.

Figure 2: Schematic of the laser processing set-up.

CHARACTERISATION
❑ Samples were polished and etched using glyceregia to reveal the grain boundaries
❑ Microstructure analysis was carried out using a scanning electron microscope (SEM)
❑ Surface mean value roughness (Ra) measurements were performed using a stylus profilometer according to ISO 4287/4288.
❑ Surface temperature predictions were made using [7,8]:

$$T(z,t) = T_0 + \frac{AP}{2k\pi V_b \sqrt{t(t_i+t_0)}} \left[\exp\left\{ -\frac{(z+z_0)^2}{4\alpha t} \right\} + \exp\left\{ -\frac{(z-z_0)^2}{4\alpha t} \right\} \right] \operatorname{erfc}\left(\frac{z+z_0}{\sqrt{4\alpha t}} \right) \qquad \text{Eq. 1}$$

RESULTS

MICROSTRUCTURE AND TEMPERATURE DISTRIBUTION ANALYSIS

❑ Figure 3 illustrates the surface melting induced by the laser treatment at increasing energy fluence. The surface temperature directly under the surface was estimated, using Equation 1, to be approximately 1190, 2001 and 3111K for figures 3 and 4(a)(b)(c) respectively.
❑ Figure 3(a) show laser marking features with localized melting effects and the corresponding figure 4(a) highlights a low depth of processing. No grain structure changes are visible in figure 4(a) with only heat affected zones visible without any valid evidence of melting of the surface.
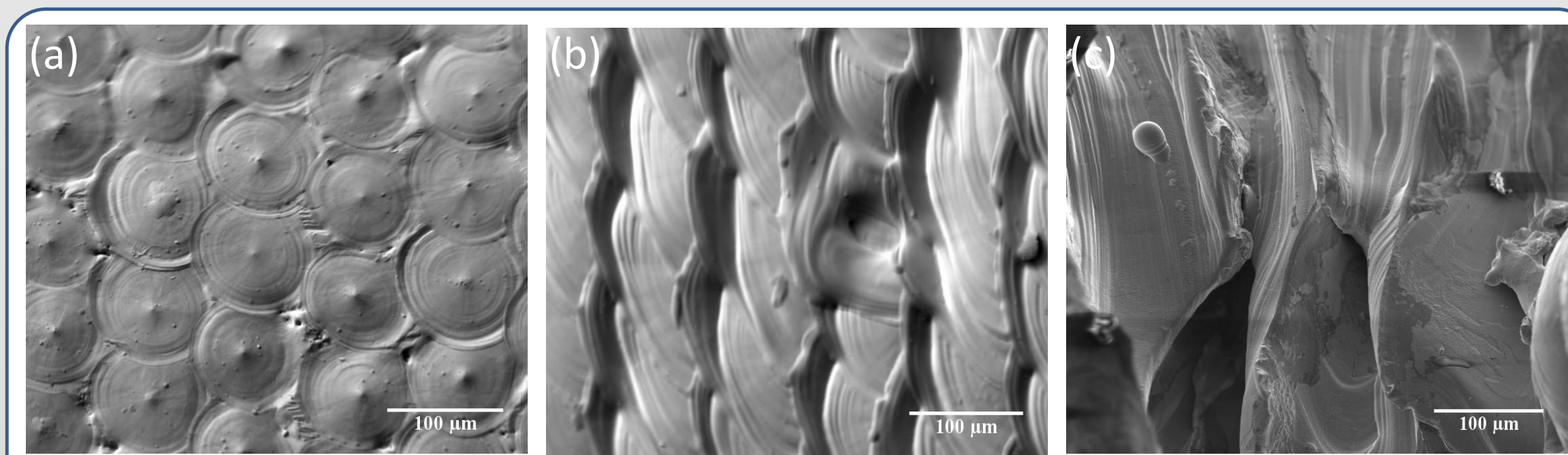

Figure 3: Effects of energy fluence on surface melting (a) 524J/cm^2, (b) 1048J/cm^2 and (c) 2096J/cm^2.
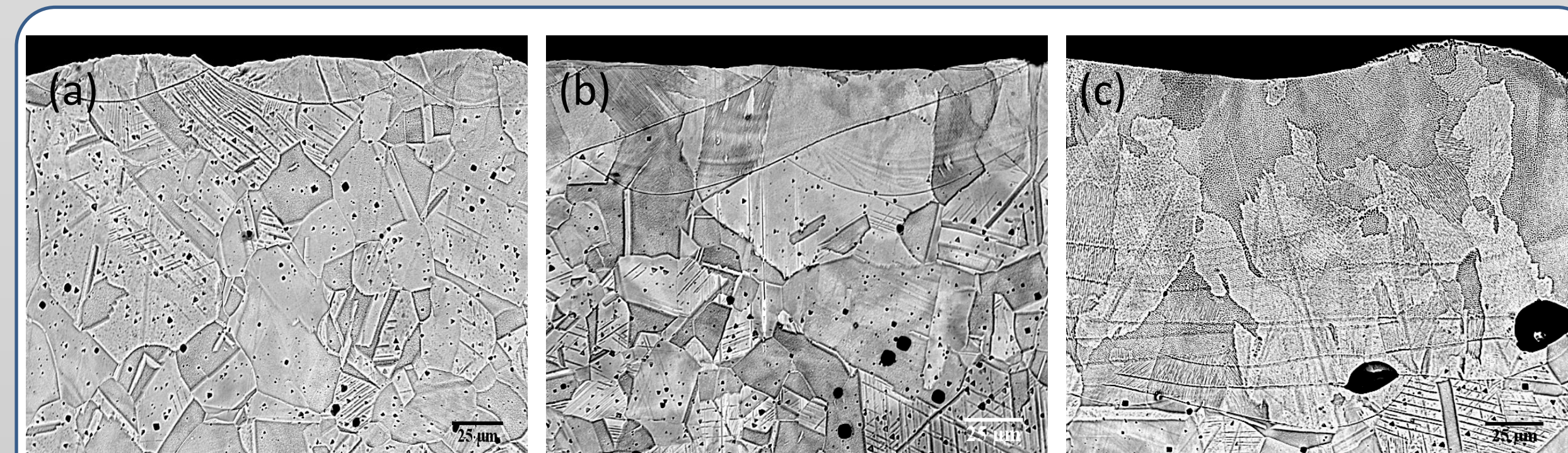

Figure 4: Back scatter SEM images of transverse cross sectional microstructure corresponding to processed surface shown in Figure 3 (a), (b) and (c).

❑ At ~2000K, figures 3(b) and 4(b) illustrate homogenised melting with increased depth of processing and overlapping becoming visible.
❑ The overlapping effect represent melt pools wider than the original spot size resulting in subsequent laser pulse directly irradiating the previous melt pool or heated region. The temperature gradient and different cooling rates forged a boundary creating overlaps visible in figure 3(b). Centrifugal force due to sample rotation was also a significant contributing factor to the overlapping features observed on the microstructural images.
❑ Figures 3(c) and 4(c) depict the surface and cross-section microstructure at an energy fluence approximately 4 times larger than (a) with surface temperature approximately 3111K. An increased depth of processing is observed, while other region highlights ablation due to increased irradiance values. Grain size and orientation is significantly altered.

MELT POOL SIZE AND ROUGHNESS ANALYSIS

❑ Figure 5 highlights the effects of residence time on the depth of processing at varying irradiance values. Augmentation in melt pool depth is fairly linear with increasing residence time for all irradiance values.
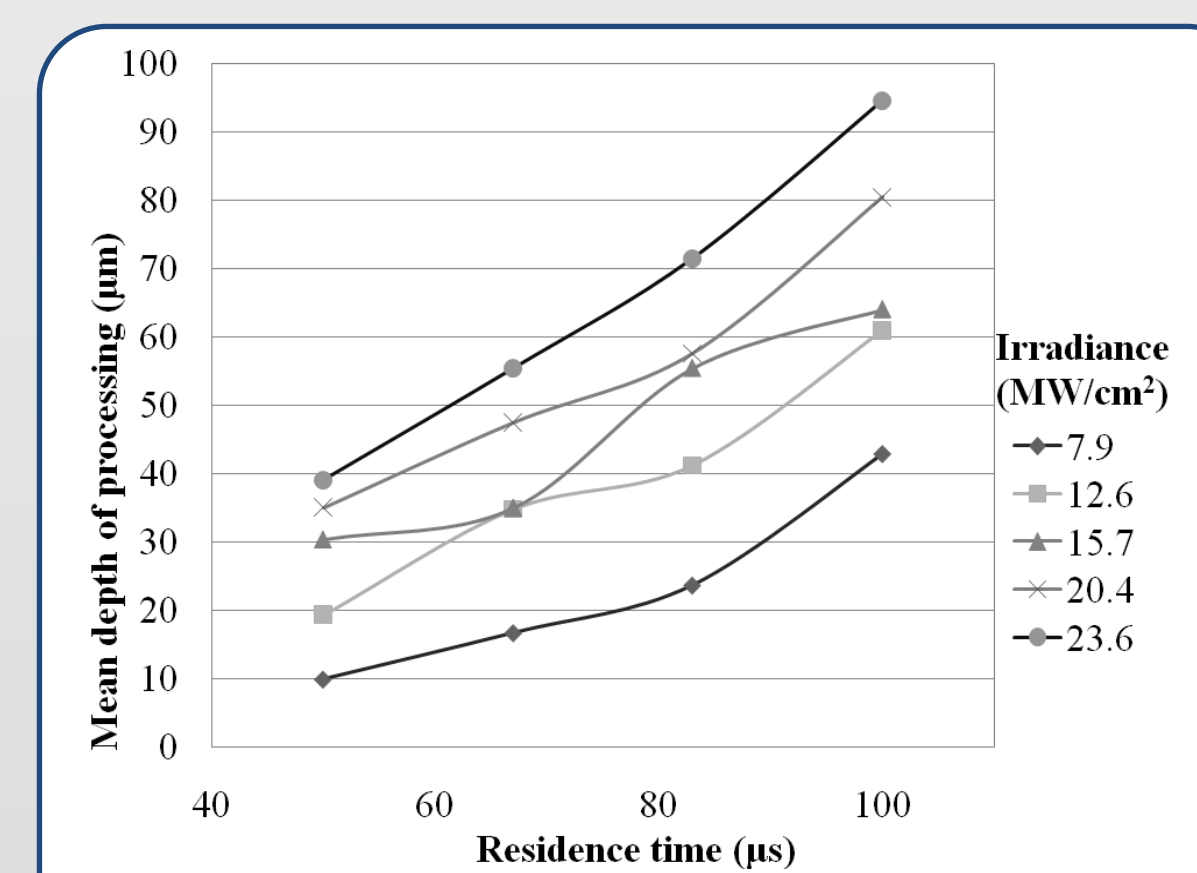

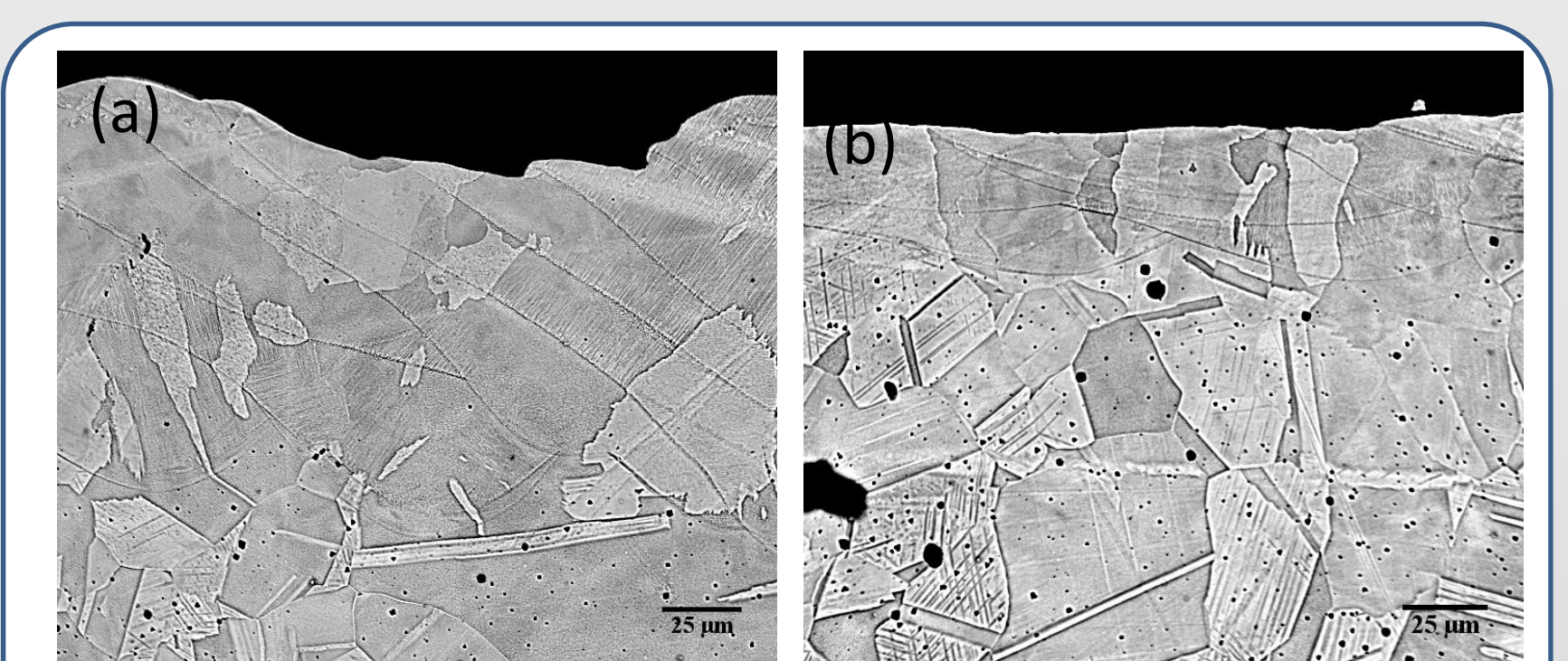Figure 5: Effects of Irradiance and residence time on melt pool depth

Figure 6: Back scatter SEM cross section micrographs of samples processed using the same energy fluence (1310J/cm^2) with: (a) low peak power (0.5kW) and high residence time (167µs); (b) high peak power (1kW) and low residence time (83µs)

❑ The morphology exhibited in 6(a) showed increased melted phase with high melt pool depth due to a higher residence time. Despite the energy fluence being similar lower residence time produced less surface melting and hence a smoother surface morphology. This is evident from the roughness results shown in figure 7 .
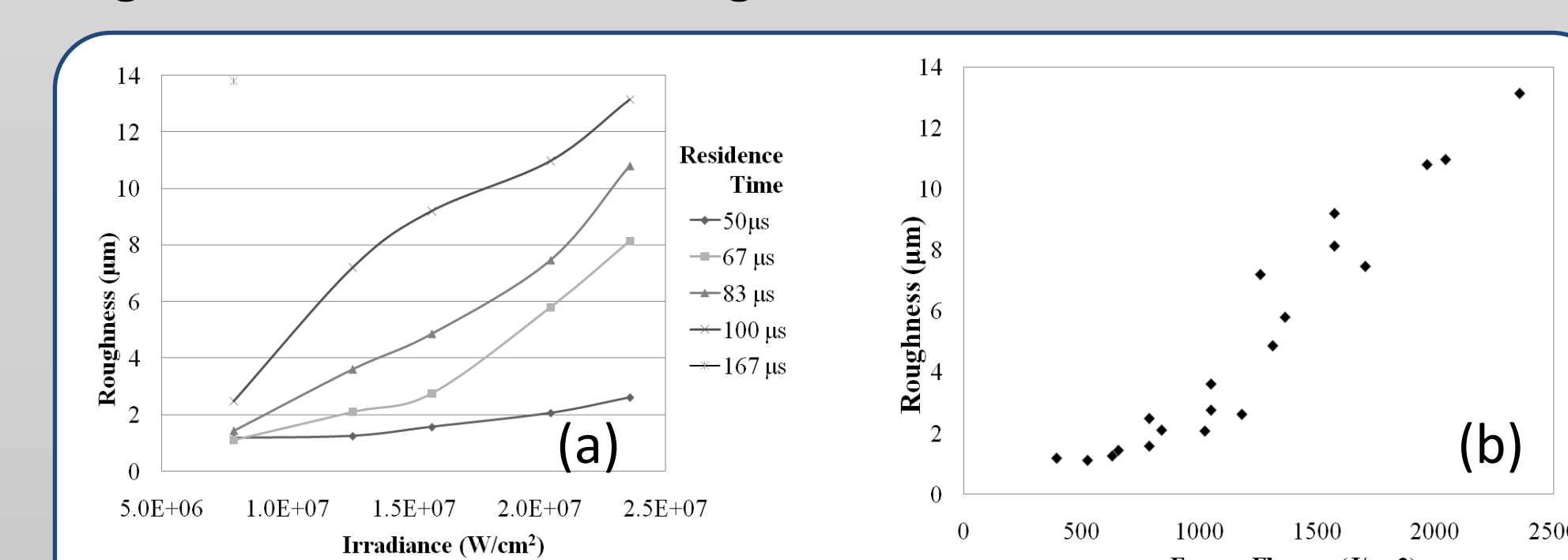

Figure 7: Relationship between average surface roughness and (a) Irradiance at varying residence times (b) Energy fluence
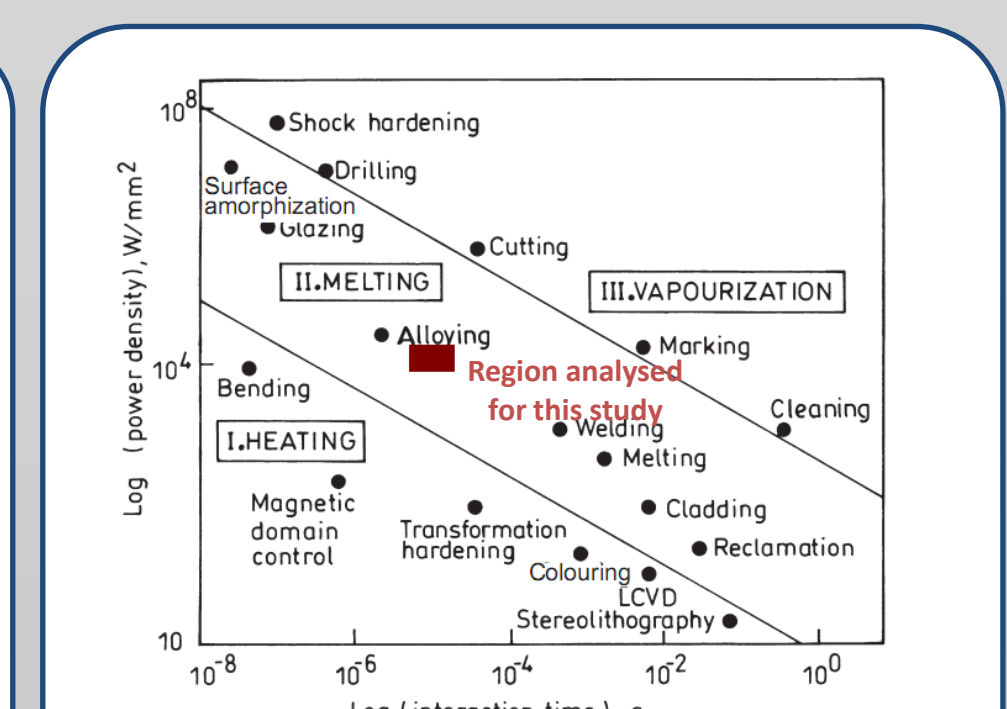

Figure 8: Regimes of irradiance and interaction time for various laser processing methods [5]

❑ Surface roughness is related to the irradiance and residence time. Figure 7(a) shows an Increase occurring with elevation of both parameters. A strong correlation is also visible between roughness and energy fluence used in the experiment regardless to the exposure time; see Figure 7(b). The first three points on the graph represent regions not melting due to low energy fluence.
❑ Figure 8 highlights the parameters used for this study. To obtain a significant change in surface tribological properties the interaction time has to be reduced while increasing the power density.

CONCLUSIONS

❑Low energy fluence (less than 629J/cm^2) had no melting effect on the surface of the stainless steel regardless of the irradiance and residence times used; no physical change in grain structure was detected
❑Medium level energy fluence approximately 1048J/cm^2 produced uniform melting on the surface with melt pool depth reaching approximately 60µm and visible overlapping induced by increased melting areas larger than the laser spot size
❑High levels of energy fluence, exceeding 2096J/cm^2, produced changes in grain size and orientation and higher depth of processing (up to ~130µm). Larger grains were also observed in the processed regions and evidence of ablation visible on the surface. Roughness and melt pool depth increased with higher levels of both irradiance and residence time
❑ No crystalline changes were observed and this is mostly like due to high residence time used in the experiment.

REFERENCES

[1] Hao, L., (2005), *Laser surface treatment of bio-implant materials,* Wiley, c2005.
[2] Dearnley, P.A. (1999), *Proc. of the Inst. of Mech. Eng. Part H,* Vol.213, pp. 107-135.
[3] Steen, W.M. and Watkins, K.G., (1993), *Journal De Physique IV,* Vol.3 pp. 581.
[4] Majumdar, J.D., et al., (2004), *Surface and Coatings Tech.,* Vol.179, pp. 297-305.
[5] Majumdar, J.D. and Manna, (2003), "Laser processing of materials", *Sadhana,* Vol.28, pp.495–562.
[6] Mahank, T., (2004), "Laser glazing of metals and metallic and ceramic coatings", thesis, pp. 26
[7] Ready, J.F. and Farson, D., (2001), *LIA handbook of laser materials processing,* LIA
[8] Selvan, J.S., Soundararajan, G. and Subramanian, K., (2000), *Surface and Coatings Technology,* Vol.124 (2-3), pp. 117-127.